Circulation: Arrhythmia and Electrophysiology

ORIGINAL ARTICLE

Evaluation of ECG Imaging to Map Hemodynamically Stable and Unstable Ventricular Arrhythmias

Adam J. Graham, MD*; Michele Orini, PhD*; Ernesto Zacur, PhD; Gurpreet Dhillon, MD; Holly Daw, BSc; Neil T. Srinivasan, MD, PhD; Claire Martin, MD, PhD; Jem Lane, MD, PhD; Josephine S. Mansell, MD; Alex Cambridge, BSc; Jason Garcia, BSc; Francesca Pugliese, MD, PhD; Oliver Segal, MD; Syed Ahsan, MD; Martin Lowe, MD, PhD; Malcolm Finlay, MD, PhD; Mark J. Earley, MD; Anthony Chow, MD; Simon Sporton, MD; Mehul Dhinoja, MD; Ross J. Hunter, MD, PhD; Richard J. Schilling, MD; Pier D. Lambiase, MD, PhD

BACKGROUND: ECG imaging (ECGI) has been used to guide treatment of ventricular ectopy and arrhythmias. However, the accuracy of ECGI in localizing the origin of arrhythmias during catheter ablation of ventricular tachycardia (VT) in structurally abnormal hearts remains to be fully validated.

METHODS: During catheter ablation of VT, simultaneous mapping was performed using electroanatomical mapping (CARTO, Biosense-Webster) and ECGI (CardioInsight, Medtronic) in 18 patients. Sites of entrainment, pace-mapping, and termination during ablation were used to define the VT site of origin (SoO). Distance between SoO and the site of earliest activation on ECGI were measured using co-registered geometries from both systems. The accuracy of ECGI versus a 12-lead surface ECG algorithm was compared.

RESULTS: A total of 29 VTs were available for comparison. Distance between SoO and sites of earliest activation in ECGI was 22.6, 13.9 to 36.2 mm (median, first to third quartile). ECGI mapped VT sites of origin onto the correct AHA segment with higher accuracy than a validated 12-lead ECG algorithm (83.3% versus 38.9%; P=0.015).

CONCLUSIONS: This simultaneous assessment demonstrates that CardioInsight localizes VT circuits with sufficient accuracy to provide a region of interest for targeting mapping for ablation. Resolution is not sufficient to guide discrete radiofrequency lesion delivery via catheter ablation without concomitant use of an electroanatomical mapping system but may be sufficient for segmental ablation with radiotherapy.

VISUAL OVERVIEW: A visual overview is available for this article.

Key Words: catheter ablation ■ consensus ■ electrodes ■ magnetic resonance imaging ■ tachycardia, ventricular

Clinical outcomes for catheter ablation of ventricular tachycardia (VT) remain suboptimal despite advances in mapping technology.[1] Mapping is frequently limited by hemodynamic instability, hence substrate-based ablation strategies have been developed to combat this with varied results due to lack of consensus in the criteria for targeting proarrhythmic sites and limitations of lesion delivery.[2] The ability to accurately and expediently map exit sites in unstable VT could offer promise to improve outcomes and the efficiency of procedures.[3]

See Editorial by Sapp et al

Correspondence to: Pier D. Lambiase, MD, PhD, Department of Cardiology, UCL Institute of Cardiovascular Science, Barts Heart Centre, Barts Health NHS Trust, W Smithfield London, EC1A 7BE, United Kingdom. Email p.lambiase@ucl.ac.uk

*A.J. Graham and Dr Orini contributed equally to this work.

The Data Supplement is available at https://www.ahajournals.org/doi/suppl/10.1161/CIRCEP.119.007377.

For Sources of Funding and Disclosures, see page 164.

Circulation: Arrhythmia and Electrophysiology is available at www.ahajournals.org/journal/circep

WHAT IS KNOWN?

- ECG imaging allows noninvasive reconstruction of epicardial unipolar electrograms using heart-torso geometry and body surface potentials in just 1 beat.
- The ECG imaging system has been recently introduced for clinical application, and its accuracy has not been quantitatively assessed with simultaneous recordings during catheter ablation for ventricular tachycardia.

WHAT THE STUDY ADDS?

- ECG imaging outperforms the standard 12-lead surface ECG for localization of ventricular tachycardia circuits during ventricular tachycardia ablation.
- The ECG imaging system localizes sites of origin of ventricular tachycardia with a resolution of 22.6, 13.9 to 36.2 mm. A resolution that is insufficient to solely guide catheter ablation of ventricular tachycardia but potentially sufficient for noninvasive radiation therapy.

Nonstandard Abbreviations and Acronyms

AT	activation time
EAM	electroanatomical mapping
ECGI	ECG Imaging
LV	left ventricle
RV	right ventricle
SoO	sites of origin
VT	ventricular tachycardia

Electrocardiographic imaging (ECGI) employs body surface electrodes combined with a patient-specific computed tomography or magnetic resonance imaging–derived epicardial geometry to display the full sequence of electrical activity during a single beat over the whole heart, hence providing a panoramic map of the arrhythmia.[4] This is achieved using an inverse method described and tested in prior publications[5–7] and commercial ECGI systems, for example, CardioInsight, have recently become available for clinical applications. This commercial system uses the method of fundamental solutions to solve the inverse problem of electrocardiography. Other methods have been developed, attempting to correct for inhomogeneities between the epicardial surface and body surface, with as yet no improvement in accuracy.[8]

Clinically, ECGI has been utilized in ablation of ventricular ectopy[9,10] and a noncommercial research-oriented ECGI system has been used most recently to direct stereotactic body radiation therapy, in failed radiofrequency ablation VT cases.[11,12] However, there has been limited study of arrhythmias in structural heart disease and limited simultaneous validation during VT.[13] Following an initial study focusing on simultaneous comparison of ECGI derived versus contact-mapping measured unipolar electrogram and activation/repolarization maps,[14] we studied the accuracy of the commercially available ECGI system CardioInsight in mapping hemodynamically stable and unstable VT using contact electroanatomical mapping (EAM) data collected simultaneously as a reference.

METHODS

Because of the sensitive nature of the data collected for this study, requests to access the dataset from qualified researchers trained in human subject confidentiality protocols may be sent to Professor Pier Lambiase, UCL, London at p.lambiase@ucl.ac.uk.

The study was approved by the National Research Service Committee, London (14/LO/0360). Thirty-seven patients undergoing catheter ablation of VT were recruited for the study. Ten of these were elective, with the remaining being emergency procedures. All patients were scheduled for a catheter ablation on clinical grounds for structurally abnormal heart VT and gave their informed consent to participate in the research study.

Clinical Method

Procedures were performed under conscious sedation using Diamorphine and Midazolam or general anesthetic. Endocardial access was obtained under ultrasound guidance using Seldinger technique via the right femoral vein±right femoral artery. All patients were planned for endocardial access to the right ventricle (RV)±left ventricle (LV) access via trans-septal puncture or retrogradely via the aorta. A subxiphisternal puncture using a Tuohy needle, with fluoroscopic guidance, was used to access the epicardial space in 5 patients, using a previously described technique.[15]

A full geometry of the ascending, arch, and descending aorta was created for co-registration with ECGI (Figure 1A). If arterial access was not part of the procedure, detailed geometry from either the right ventricular outflow tract and the inferior and superior vena cava, or the left atrium was collected (Figure 1B).

Ventricular tachycardia was induced with a standard Wellens protocol from the RV apex. If no VT was induced, the protocol was repeated from the right ventricular outflow tract or LV. An EAM (CARTO, Biosense-Webster, CA) was created during VT using a multipolar catheter or by point-by-point mapping (Pentarray, Decapolar or SmarTouch, Biosense-Webster, CA). In hemodynamically tolerated VTs, identification of sites of origin (SoO) was defined by entrainment or termination with ablation. Entrainment at a cycle length 20 ms shorter than the VT was attempted at sites where diastolic activity was seen. For the purpose of the study, a rhythm was considered entrained when concealed fusion with a postpacing interval minus tachycardia cycle length of <30 ms was present and the S-QRS was <50% of the tachycardia cycle length.[16] In the case of unstable VT or nonsustained VT, pace-mapping was performed and the average correlation coefficient between the 12-lead ECG of VT and the paced beat was calculated using the Bard EP system (Boston Scientific, MA). An average correlation coefficient

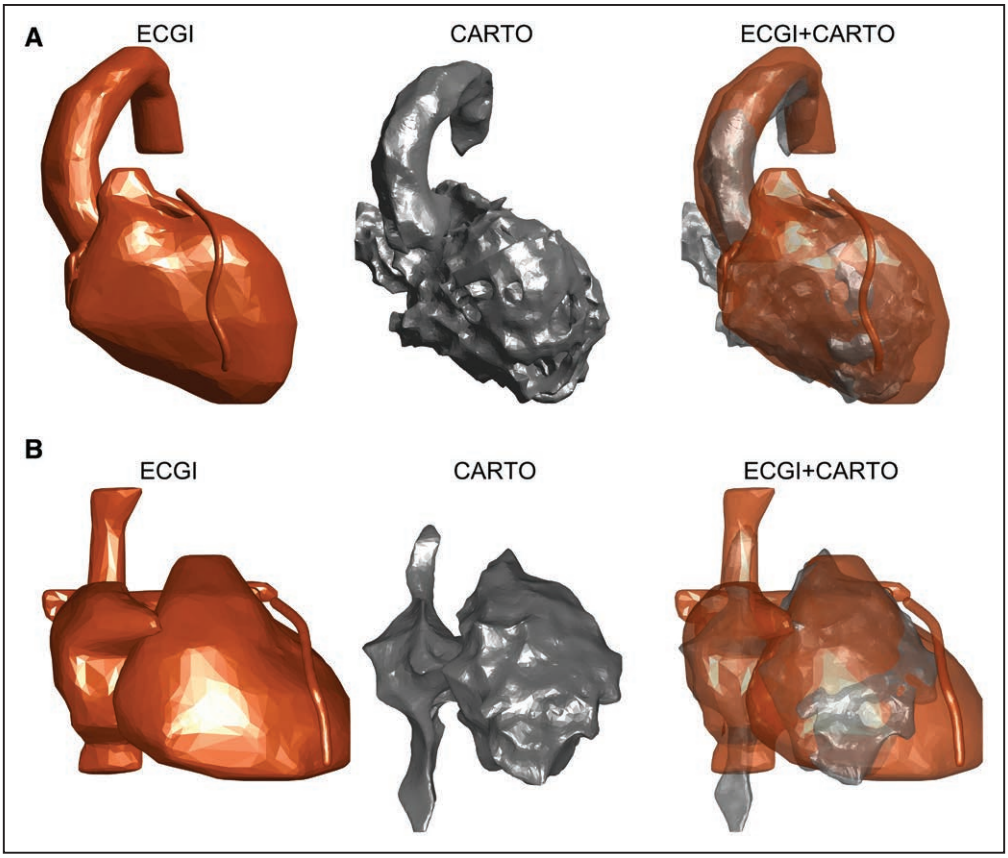

Figure 1. Anatomic co-registration of ECG imaging (ECGI; left) and CARTO (middle) geometries in 2 patients. The 2 geometries are combined in the panel on the right. **A**, Demonstrates the use of the aorta for co-registration and in (**B**) the right ventricular outflow tract, inferior vena cava, and superior vena cava.

≥90% was taken as a surrogate marker of the VT SoO/exit zone.[17] The location on the EAM of these sites was recorded.

ECGI

Before catheter ablation, a 252-electrode vest (CardioInsight, Medtronic, MN) was fitted for recording of body surface potentials (sampling rate, 1000 Hz) and remained in situ until conclusion of the procedure. A noncontrast axial computed tomography scan with 3 mm slice thickness was performed up to 4 hours before the procedure. Patient-specific epicardial geometry was created using the EcVue system (Medtronic, MN) with data from the computed tomography and body surface potentials. Epicardial unipolar electrograms were computed over ≈1400 epicardial points covering both ventricles using torso-heart geometry and unfiltered body surface potentials. Reconstructed unipolar electrograms over the atrioventricular valves were excluded from the analysis. Activation time (AT) and voltage maps were created for all induced VTs.

Co-registration of EAM and ECGI geometries was performed semiautomatically with bespoke software (Matlab, The Mathworks, Inc, MA) as in our previous study.[14] Figure 1 shows alignment of ECGI and EAM geometries including the Aorta, left atrium and inferior vena cava, and right ventricular outflow tract. The optimal co-registration was visually determined by 2 experts independent of subsequent analysis.

The VT SoO was projected from the co-registered EAM onto the nearest node of the ECGI geometry, including for SoO localized to the septum.

Unipolar electrograms from ECGI were analyzed blindly to VT SoO (Matlab, The Mathworks, Inc, MA). Signals were band-pass filtered between 0.5 and 80 Hz and AT was measured as the time of the steepest signal downslope (dV/dt_{min}) during the QRS complex.[18,19] In ECGI, multiple sites may share the same AT. Therefore, the site of the earliest activation was defined as the nearest site to the center of the region of earliest activation (area including 2% of sites showing earliest activation). The closest site to the center of the area of earliest negative voltage was also utilized to localize earliest sties of activation.[20] This was defined as the area including the first 2% of sites showing a voltage lower than a patient-specific noise threshold (1/3 of the absolute minimum potential).

The Euclidean distance between the VT SoO and the earliest activation sites on ECGI was calculated to assess ECGI spatial resolution for VT mapping.

All signals and markers were carefully reviewed and semi-automatically corrected if needed as in previous studies.[21,22]

12-Lead ECG Comparison

Twelve lead body surface ECGs were recorded throughout the cases using Bard EP system (Boston Scientific, MA) with filters set between 0.5 and 100 Hz. A contemporary algorithm that allocates the VT SoO to one of the 17 myocardial segments of the standard AHA model was implemented.[23] The ECGs for each mapped VT were analyzed by 2 experts who allocated the SoO onto the corresponding cardiac segment by following the algorithm. A third electrophysiologist arbitrated any discrepancies. Both were blinded to results of EAM and ECGI

maps. ECGI and EAM were allocated a segment based on the position of the earliest site of activation and the SoO, on ECGI and EAM, respectively, with the central point in the region of earliest activation used for ECGI. Given ECGI reconstructs epicardial potentials only, VTs with a septal SoO on the EAM were excluded from the 17-segment model comparison portion of the analysis. SoO from the RV were also excluded as they are not part of the AHA 17 segment model.

Statistical Analysis

Data distribution is described by median, first-third quartiles. Statistical differences were assessed using the Wilcoxon rank-sum test for unpaired comparisons and the Wilcoxon signed-rank test for paired comparisons. Differences between the proportion of correct cardiac segments identified by ECGI or 12-Lead ECG were assessed using the exact Fisher test. Threshold for statistical significance was 0.05. Statistical analysis was performed in Matlab, MathWorks.

RESULTS

Nineteen of the 37 patients prospectively recruited were excluded from the final analysis. Five were non-inducible (26.3%), 3 due to procedural complications (15.8%), 1 due to ECGI equipment failure (5.3%), and 10 on account of hemodynamically nontolerated VT with no suitable pace-mapping (52.6%). Absence of pace-mapping was on account of inability to pace from areas producing adequate morphology match or due to termination of case before pace-mapping was employed. Procedural complications were unrelated to ECGI. One patient had a groin complication, 1 a large pericardial effusion during epicardial access, and 1 became hypotensive during the procedure.

Eighteen patients were studied, of which 4 had dilated cardiomyopathy (22.2%), 4 arrhythmogenic RV cardiomyopathy (22.2%), and 10 ischemic heart disease (55.6%) (Table 1). Twenty nine different VT circuits mapped using EAM of which 20 (69%) where hemodynamically stable and 9 (31%) unstable. Epicardial access was utilized in 5 patients (27.8%). Three VTs were mapped to the epicardium (10%) and 26 (90%) to the endocardium. Of the endocardial VTs, 6 were localized to the septum (5 LV and 1 RV) and 6 the RV. The remaining were mapped to the LV anterior, inferior, or lateral walls. The SoO was located with entrainment in 11 VTs (38%), termination with ablation in 9 VTs (31%), and pace mapping in 9 VTs (31%). If a rhythm was entrained and then subsequently terminated with ablation, for the purpose of analysis this was recorded as entrained (Table 2).

ECGI Localization of VT Circuits

Co-registration of ECGI and EAM geometries utilized the Aorta in 11 patients (61.1%), left atrium in 4 patients (22.2%), and inferior vena cava and right ventricular outflow tract in 3 patients (16.7%).

Of the 11 entrained VTs, 9 (81.9%) presented lines of block adjacent to the region of earliest activation (Figure I in the Data Supplement). In general, however, the VT circuit, which could involve intramural pathways, was not discernible from ECGI AT maps. In the region of earliest

Table 1. Baseline Characteristics for Patients Included in Analysis

Patient	Age (y)	Sex	Etiology	ICD	LVEF (%)	Antiarrhythmics	Anatomic Structure
1	73	M	IHD	Y	20	Bisoprolol, amiodarone	Ao
2	22	M	ARVC	N	>55	Bisoprolol	RVOT, SVC, IVC
3	43	M	ARVC	Y	>55	Sotalol	Ao
4	54	M	DCM	Y	>55	Bisoprolol, amiodarone	Ao
5	81	M	IHD	Y	25	Bisoprolol, amiodarone, mexiltine	Ao
6	82	M	IHD	Y	22	Bisoprolol, amiodarone	LA
7	76	F	IHD	Y	20	Bisoprolol, amiodarone	Ao
8	24	F	ARVC	N	>55	Flecainide	RVOT, SVC, IVC
9	79	M	IHD	Y	30	Bisoprolol, amiodarone, mexiltine	Ao
10	78	M	IHD	Y	15	Bisoprolol, amiodarone	Ao
11	55	M	DCM	Y	45	Sotalol	LA
12	78	M	IHD	Y	14	Bisoprolol	Ao
13	69	M	IHD	Y	10	Bisoprolol, amiodarone	Ao
14	79	M	IHD	Y	25	Bisoprolol, mexilitine	LA
15	82	M	DCM	Y	45	Bisoprolol, amiodarone	LA
16	52	F	ARVC	Y	>55	Sotalol	RVOT, SVC, IVC
17	22	M	DCM	Y	40	Bisoprolol, amiodarone	Ao
18	84	M	IHD	Y	20	Bisoprolol, mexilitine, amiodarone	Ao

Ao indicates aorta; ARVC, arrhythmogenic right ventricular cardiomyopathy; DCM, dilated cardiomyopathy; F, female; ICD, implantable cardioverter-defibrillator; IHD, ischemic heart disease; IVC, inferior vena cava; LA, left atria; LVEF, left ventricular ejection fraction; M, male; RV, right ventricular; RVOT, right ventricular outflow tract; and SVC, superior vena cava.

Table 2. Localization of VT SoO Using ECGI

VT	Pts	Localization of VT SoO	ENTR	ABL	PM	Distance to VT SoO (mm)	AHA Segment ECGI	AHA Segment 12-L ECG
1	1	LV basal anteroseptal			✓	25.4	N/A	N/A
2	1	LV basal anterior			✓	37.5	✓	✓
3	2	RV inferior			✓	19.7	N/A	N/A
4	3	RV lateral wall	✓			13.3	N/A	N/A
5	4	RVOT	✓			35.8	N/A	N/A
6	5	LV basal inferolateral	✓			35.1	✓	×
7	5	LV basal inferior	✓			39.4	✓	×
8	5	LV basal anterior		✓		67.1	×	✓
9	5	LV mid inferolateral		✓		23.6	✓	×
10	5	LV basal inferolateral	✓			39.0	✓	×
11	6	LV mid inferolateral		✓		39.5	×	✓
12	7	LV mid anteroseptal		✓		54.5	N/A	N/A
13	8	LV mid anterior (EPI)		✓		14.2	✓	✓
14	8	RVOT	✓			7.4	N/A	N/A
15	9	LV mid inferolateral		✓		4.1	✓	×
16	9	LV basal inferolateral	✓			25.1	✓	×
17	10	LV mid anterior	✓			32.3	×	×
18	10	LV mid anterolateral		✓		26.6	✓	×
19	11	RV septum	✓			3.4	N/A	N/A
20	11	LV basal anteroseptal	✓			10.7	N/A	N/A
21	11	LV basal anteroseptal	✓			20.6	N/A	N/A
22	12	LV mid inferolateral			✓	17.0	✓	×
23	13	LV mid anterior			✓	6.9	✓	✓
24	14	LV mid anteroseptal			✓	14.1	N/A	N/A
25	15	LV basal anterior		✓		22.6	✓	×
26	15	LV basal anterior			✓	8.5	✓	✓
27	16	LV RV free wall (EPI)			✓	76.2	N/A	N/A
28	17	LV mid inferolateral (EPI)			✓	17.3	✓	✓
29	18	LV mid anterior		✓		19.1	✓	×
			n=11 (38%)	n=9 (31%)	n=9 (31%)	22.6 (14–36)	n=15 (83%)	n=7 (39%)

SoO was determined by pace-mapping (PM), entrainment (ENTR), or termination with ablation (ABL). Distance to VT SoO: distance from the site of earliest activation on ECGI to the VT SoO registered on the EAM. Indication of whether the correct anatomic segment of the VT SoO was identified by ECGI or by a 12-lead ECG algorithm is given by ✓: Match. ×: no Match. N/A: not available (RV and septal VTs were excluded as not represented either in AHA or ECGI). EAM indicates electroanatomical map; ECGI, ECG imaging; RV, right ventricular; SoO, site of origin; and VT, ventricular tachycardia.

activation, the ECGI unipolar electrograms showed a QS complex typical of the earliest activation independent of endocardial as opposed to epicardial origin (Figure II in the Data Supplement).

Figures 2–4 show examples of VTs terminated with ablation, pace-mapped, and entrained, respectively.

The distance between the site of earliest activation on ECGI and the nearest ECGI point to the VT SoO registered on EAM was 22.6, 13.9 to 36.2 mm (median, first to third quartile; Table 2). This was not significantly different between VTs that were pace-mapped, entrained, or terminated with ablation ($P>0.3$), or between VTs mapped on the RV versus LV ($P=0.47$), while borderline nonsignificant differences existed between ischemic (26.6, 18.5–39.1 mm) and nonischemic patients (15.8, 9.6–21.6 mm), $P=0.055$. In 7 patients, more than 1 VT was mapped, with an average distance per patient of 18.2, 14.8 to 34.7 mm. In 2 of the 3 VTs mapped onto the epicardium, distance from the earliest site of activation in ECGI and VT SoO was lower than the median (14.2 and 17.3 mm), whereas in the remaining case, the distance was much larger as in this case ECGI showed 2 distinct regions of earliest activation, with the earliest being located on the opposite site of the heart.

Using time to earliest negative voltage instead of AT to define the earliest site of activation provided significantly lower resolution, with distance from VT SoO equal to 34.6, 18.8 to 45.4 mm ($P=0.039$).

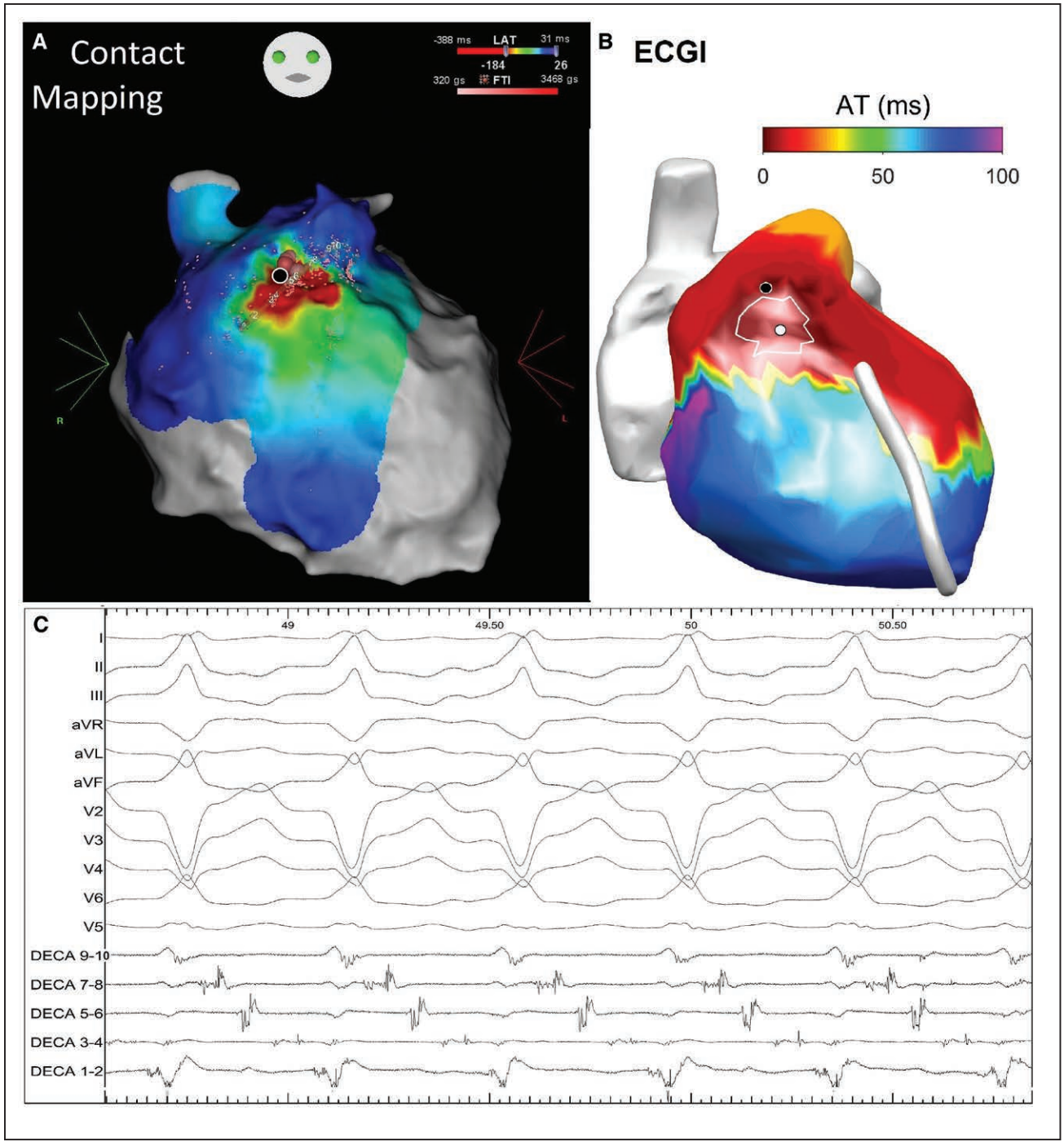

Figure 2. Example from a ventricular tachycardia (VT) terminated with ablation.
A, Contact electroanatomical map (EAM) of a VT (patient #8, VT #13) shown in anteroposterior (AP) view. The red coloured area denotes diastolic activity seen on a decapolar catheter overlying this area, with bipolar electrograms (EGMS) from this shown in **C**. Ablation tags (shown as red spheres) can be seen above the decapolar catheter, with the black circle highlighting the point from where VT was terminated during ablation. **B**, ECG imaging (ECGI) activation time (AT) map, shown in AP view, of the same VT. The area of the earliest activation (lowest 2% of AT) is bordered by a white line and a white circle highlights its geometric center, which is the earliest site of activation. A black circle represents the nearest ECGI site to the VT site of origin registered on the contact EAM. **C**, Surface ECG and intracardiac bipolar EGMs taken from decapolar catheter position as seen in (**A**). Entrance to the isthmus can be seen on decapoles 7 to 8 with electrogram timing progressively later during the diastolic period until probable exit site in 1 to 2.

Table I in the Data Supplement shows results of further analysis, including distance from the site of earliest activation in ECGI to the original VT SoO registered on the EAM (without projecting it onto the nearest ECGI point) of 26.1, 13.9 to 36.2 mm and distance from the VT SoO to the margin of the area of earliest activation (surface 3.4, 1.8–4.3 cm^2) of 13.0, 3.4 to 24.0 mm.

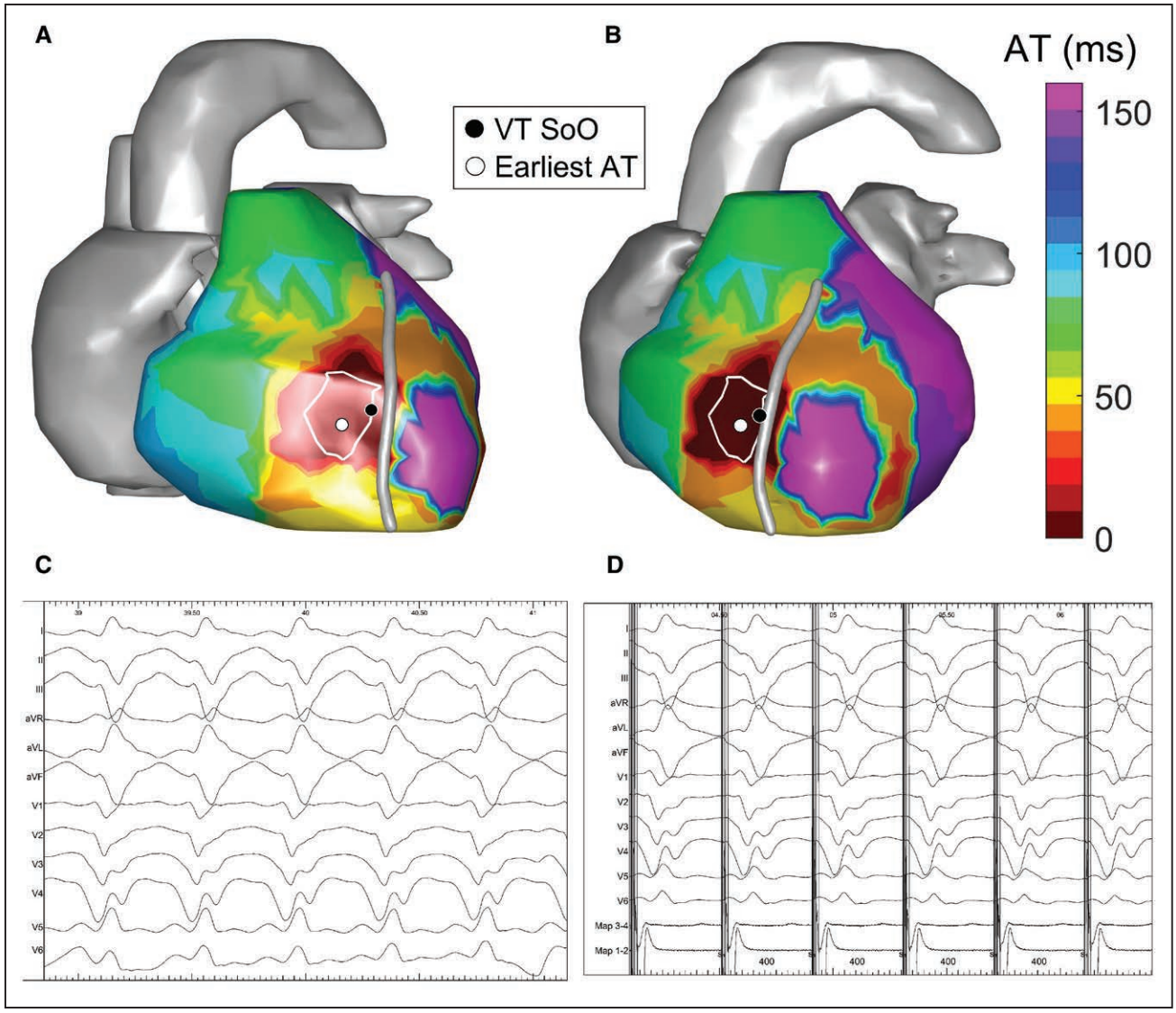

Figure 3. Example from a pace-mapped ventricular tachycardia (VT; patient #14, VT #24).
Top: ECG imaging (ECGI) activation time map during VT shown in right and left anterior oblique views in (**A**) and (**B**), respectively, with atria, inferior vena cava, superior vena cava, and aorta in gray. The region of earliest activation is bordered by a white line (lowest 2% of activation time [AT]) and a white circle highlights its geometric center, which is the earliest site of activation. A black circle represents the nearest ECGI site to the VT site of origin (SoO) registered on the contact electroanatomical map and identified using pace-mapping. **C**, Surface ECG of the VT. **D**, Surface ECG during pace mapping of the VT. Paced rhythm had a 93% morphology match to the tachycardia (Template Matching, Bard EP system, Boston Scientific, MA).

ECGI localized the SoO of the VT to the correct anatomic AHA segment in 15 out of 18 cases (83.3%) whereas the 12-lead algorithm identified the correct anatomic segments in 7 out of 18 cases (38.9%); P=0.015 (see Table 2).

DISCUSSION

This is the first simultaneous assessment of an ECGI approach to localize VT sites of origin during catheter ablation in structurally abnormal hearts. Due to its spatial resolution, EAM provides a suitable reference for ECGI assessment.[24] We have demonstrated that CardioInsight localizes VT sites of origin with a spatial resolution of 22.6, 13.9 to 36.2 mm (median, first to third quartile). ECGI localized VT SoO to the correct AHA anatomic segment in 83.3% of VTs studied, outperforming a recently proposed 12-lead ECG algorithm.[23]

A recent study has questioned the accuracy of CardioInsight activation time maps, including the localization of epicardial breakthrough, during sinus rhythm.[25] Given the marked differences in conduction dynamics between sinus rhythm and re-entrant ventricular tachycardia as well as different methodological analysis, our results cannot be directly compared. One may, however, speculate that the resolution required to correctly localize the VT SoO may be lower than the resolution required to track

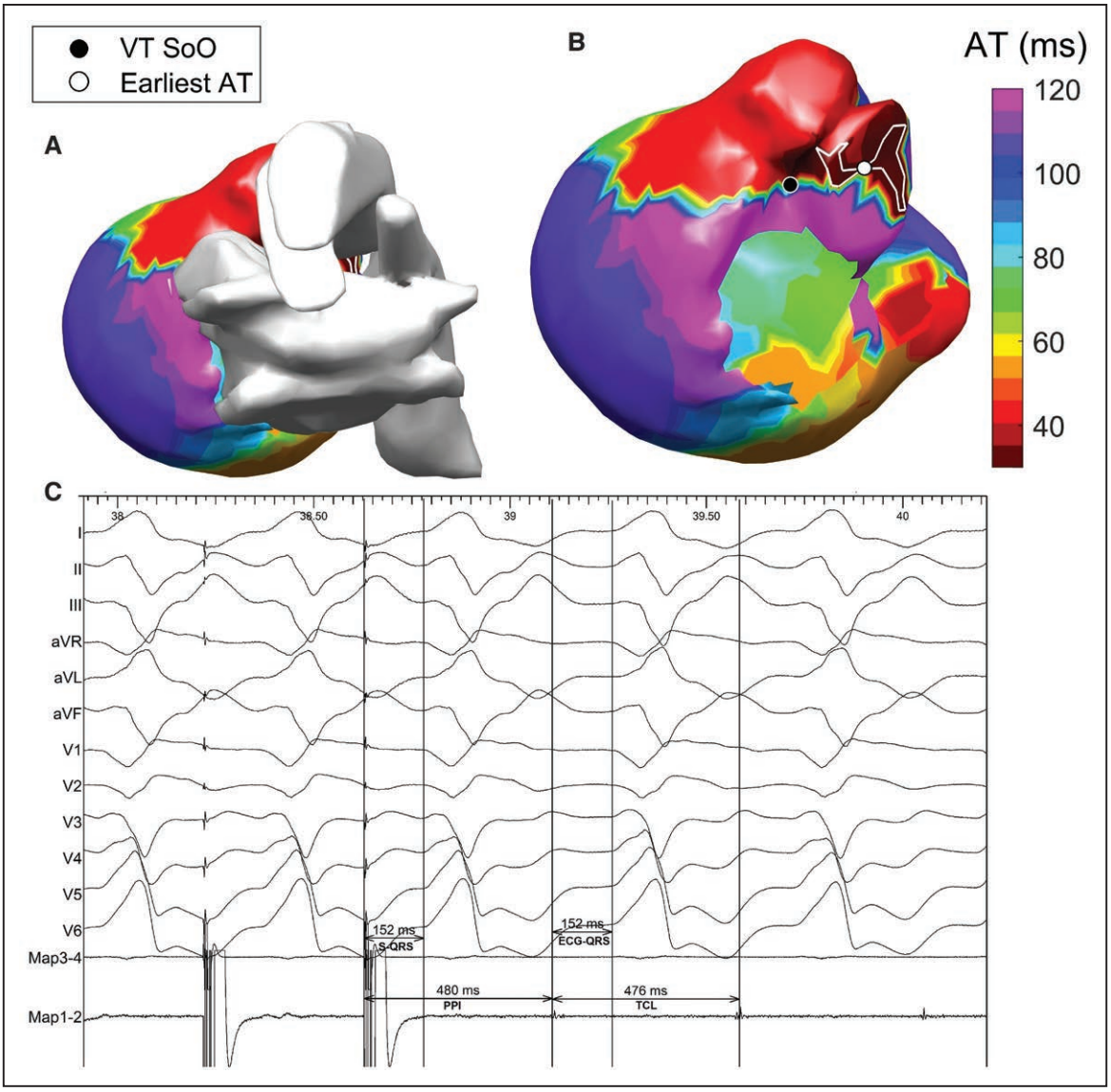

Figure 4. Example of an entrained ventricular tachycardia (VT; patient #11, VT #21).
A, ECG imaging (ECGI) activation map during VT shown in standard postero-anterior (PA) view (**A**) and a modified PA view (**B**). The region of earliest activation is bordered by a white line (lowest 2% of activation time [AT]) and a white circle highlights its geometric center, which is the earliest site of activation. A black circle represents the nearest ECGI site to the VT site of origin (SoO) registered on the electroanatomical map and identified using entrainment mapping. Activation occurs almost simultaneously on the left ventricle (LV) basal anterior wall and right ventricle basal inferior wall. Furthermore, the axis on the 12-lead ECG would suggest activation occurring from inferior to superior LV. This could be due to propagation of the re-entrant circuit exiting inferiorly from the isthmus location on the basal anteroseptum. A superior line of block would limit superior to inferior activation on the 12-lead ECG. **C**, Intracardiac electrograms demonstrating entrainment of tachycardia with a postpacing interval (PPI) minus tachycardia cycle length (TCL) of 4 ms and identical timing for stimulus to QRS (S-QRS), and local electrogram to QRS (EGM-QRS).

the activation sequence when the normal conduction system is engaged.

Previous studies have examined the capacity of ECGI to localize paced beats.[6,26–31] In experimental studies using tank-torso models, the accuracy has been shown to be <10 mm.[30,31] Similar accuracy was seen in humans when localizing RV endocardial and LV epicardial pacing from the coronary sinus.[5] Given ECGI reconstructs epicardial potentials, accuracy should be superior with direct pacing on the epicardium, when compared with endocardial pacing. However, a human study using an ECGI system based on 120-lead body-surface potential mapping reported distances to the SoO of 13.5±9 mm and a recent study from our group showed similar results.[14] In a similar study in canines using direct contact epicardial electrodes accuracy was 10 mm.[27] Although this latter study utilized a different inverse method, therefore comparison could be limited. Bear et al[32] in a porcine model utilized a similar inverse method to the one employed in our study and found an accuracy of 16 mm for localizing epicardial foci.

The localization of pacing sites provides a surrogate marker for arrhythmia localization.[4] Two studies

have examined the role of ECGI in mapping ventricular ectopy. ECGI showed superior capability to localize ventricular ectopy origins when compared with 12 lead algorithms and facilitated faster times to ablation.[9,10] For sustained VT, accurate reconstruction of activation sequences has been demonstrated in heart torso-tank models using canine hearts, where average accuracy of localization was 8.69 mm.[33] In humans, ECGI was accurate in a heterogeneous group of patients with both normal and abnormal hearts, and mainly focal VT.[13] Comparison between contact mapping and ECGI in both the VE[9,10] and VT[13] studies was based on location of an anatomic segment of the heart and not a distance to the point of earliest activation. In contrast, our data contain only structurally abnormal heart VT, with induced VTs most likely to be re-entrant in mechanism. Given the re-entrant mechanism, distance from SoO to early activation on ECGI could have been expected to be shorter for pace-mapped than entrained or terminated with ablation VTs. This was not the case in this study.

The ability to expeditiously differentiate between focal and re-entrant VTs could influence subsequent contact mapping and ablation strategy. ECGI has been shown previously to differentiate between these.[13] We found 81.8% of entrained VTs were suggestive of a macro re-entrant mechanism on ECGI, with lines of block seen in areas adjacent to areas of early activation. Although the limited number included in this study precludes definitive conclusions being drawn, in this study, ECGI did not accurately reconstruct re-entrant sequences for all VTs of this type. Figure 2 illustrates an example of accurate localization of SoO on ECGI for a re-entrant VT. The projected point from the SoO on the EAM can be seen within the area of earliest activation on ECGI. However, the direction of the propagation through the diastolic pathway on the EAM, and bipolar electrograms recorded from the decapolar catheter, would suggest activation is occurring from high to low. The ECGI map suggests the converse of this. The reasoning for this is uncertain and could represent an artefactual line of block, as has been reported by other investigators.[25,34]

ECGI is also purported to differentiate between epicardial and endocardial VT's,[13,28,31] as epicardial unipolar electrograms should exhibit an rS wave for endocardial and a pure Q wave for epicardial sites of origin. Despite being unable to directly compare accuracy of epicardial versus endocardial VTs due to insufficient data points, our findings do not support the use of ECGI to accomplish this. None of the VTs localized to the endocardium on EAM showed evidence of rS complexes in the region of early activation (see Figure II in the Data Supplement). If an endocardial site of earliest activation arising from a region of dense scar conducts epicardially, then this could explain why only Q waves are seen in a region of earliest activation on ECGI, as there is insufficient tissue to generate the electromotive force to form an R wave, hence only the epicardial breakthrough is identified as a Q wave in more superficial viable tissue. This casts doubt on ECGI being able to discern whether epicardial access is warranted based on the reconstructed electrograms from VT beats in structural heart disease.

The localization of VTs with septal origin would be expected to be less accurate as only epicardial electrograms are reconstructed. However, our data indicate that accuracy of the location of septal VTs was similar to those located elsewhere in the heart. Further data and clinical algorithm development are required to determine if ECGI can provide information on the depth of the SoO on the septum or indeed if further processing of the unipolar signals is needed to improve the identification of endo, mid-, or epicardial origins. Furthermore, we found no difference in the localization of RV and LV VTs. This is in spite of the differing wall thickness between the ventricles.

Our data demonstrated an accuracy of 83.3% with ECGI when the 17-segment model was used, which compares to over 90% accuracy in localizing mostly focal VT shown in a previous ECGI study.[13] The 12-lead ECG algorithm used for comparison in this study has been validated previously examining the 17 segment model in structural heart disease showing 81.9% of VTs localized in ischemic and nonischemic cardiomyopathy with equivalent accuracy in nonseptal VTs (83%).[23] Its applicability to various forms of heart disease was the rationale for our use of this particular algorithm. By providing more accurate localization of VT SoO than the 12 lead ECG, ECGI could better guide targeted ablation, particularly in hemodynamically unstable VT. The increased accuracy of ECGI in comparison to the 12-lead ECG could be a feature of ECGI taking into account individual heart-torso geometry and rotation, and the use of multiple body surface electrodes providing more electrical data.

This study has highlighted a number of features that could be developed to optimize the system including refinement of signal processing and algorithms for allocation of activation times to reconstructed electrograms. Indeed, additional work will be required to isolate diastolic potentials during VT if this is possible. Furthermore, integration of ECGI epicardial maps into a common geometry within an EAM system to enable targeted ablation will be a major advance. Treatment of VT using stereotactic body radiation therapy, guided in part by ECGI localization of VT, has shown promising results as VT episodes decreased from 119 (4–292) to 3 (0–31) at 6 months post-treatment.[11,12] A single segment of VT origin was targeted with a more homogenous lesion delivery versus conventional radiofrequency ablation. This novel methodology has thus far been performed in a single center and further research will be needed into both its long-term efficacy and the role played by ECGI. At present, the precision of ECGI may be sufficient to enable application of this form of energy without the need for additional

mapping as the area of lesion delivery is larger: 17 to 81 mL versus point by point radiofrequency ablation coupled with the more homogeneous tissue effects. Furthermore, ECGI localizes the VT exit site as opposed to the diastolic pathway as we are unable to discern diastolic potentials, even in the epicardial VT cases. The exit site will colocalize adjacent to the diastolic pathway in the majority of cases, which can be compensated for by a wider area of ablation of radiation energy and will also be more transmural. However, mapping of the diastolic pathway with EAM will still be required if more localized radiofrequency energy is to be delivered to the critical component of the circuit.

LIMITATIONS

There are inherent limitations posed by EAM and pacing manoeuvres to locate VT SoO. Pace-mapping accuracy can be affected by area of capture and functional block only present in VT.[16] Pace mapping was performed at the lowest outputs to ensure consistent myocardial capture but was not performed at the VT cycle length.[17] A previous study has reported 82% sensitivity and 87% specificity in identifying the exit region by pace mapping with a 82% morphology match.[17] Our choice of using a cutoff value of 90% morphology match to identify SoO is expected to provide slightly higher specificity, with a spatial resolution which needs to be assessed in future studies. Furthermore, given that ECGI reconstructs unipolar epicardial electrograms our methodology of locating SoO, mainly on the endocardium, represents an indirect comparison and introduces potential error. Points of entrainment with S-QRS interval between 30% and 50% of the tachycardia cycle length can be remote from the exit site. The inclusion of these points may have resulted in an overestimation of the distance between the VT exit site and the point of earliest activation on ECGI.[35]

Accuracy of the ECGI maps could have been affected by alterations in the relationship between the heart and torso during the cardiac and respiratory cycle.[36] To our knowledge, no adequate correction for this is currently available. Despite using fixed anatomic landmarks, the co-registration of the geometries could still introduce error. Visually, the aorta is the easiest anatomic structure to co-register and for future research, and potential clinical application, may offer the best means of effective alignment of geometries from different systems. Movements of up to 4 mm and rotations of up to 5° have been previously shown to alter correlation coefficient between activation time maps on EAM and ECGI by up to 25%.[14] An integrated ECGI and EAM system with electrogram data presented in a common geometry would overcome this issue. Finally, reported Euclidean distances could be smaller than distances accounting for the curved surface of the heart, and the statistical analysis is limited by the small number of VTs included.

CONCLUSIONS

ECGI provides sufficient resolution to identify myocardial segments with sites of earliest activation in VT but in its current iteration would be insufficient to guide catheter ablation without detailed contact mapping. However, it may be sufficient for targeting radiotherapy-based strategies or energies that deliver transmurally over a wider area than current discrete radiofrequency lesion sets. The capacity to give a region of interest could facilitate efficient targeted mapping and ablation of hemodynamically unstable VTs outperforming the 12 lead ECG.

ARTICLE INFORMATION

Received March 7, 2019; accepted November 5, 2019.

Affiliations

Barts Heart Centre, Barts Health NHS Trust, London, United Kingdom (A.J.G., M.O., G.D., H.D., N.T.S., C.M., J.L., J.S.M., A.C., J.G., F.P., O.S., S.A., M.L., M.F., M.J.E., A.C., S.S., M.D., R.J.H., R.J.S., P.D.L.), Institute of Cardiovascular Science, University College London, United Kingdom (M.O., P.D.L.). Institute of Biomedical Engineering, University of Oxford, United Kingdom (E.Z.).

Sources of Funding

A.J. Graham is supported by Barts Charity. Dr Orini is supported by British Heart Foundation grant PG/16/81/32441. Dr Lambiase is supported by UCLH Biomedicine NIHR and Barts BRC. The study was in part supported by a Medtronic External Research Program grant.

Disclosures

Dr Lambiase receives educational grants and speaker fees from Medtronic. The other authors report no conflicts.

REFERENCES

1. Josephson ME, Anter E. Substrate mapping for ventricular tachycardia: assumptions and misconceptions. *JACC Clin Electrophysiol*. 2015;1:341–352. doi: 10.1016/j.jacep.2015.09.001
2. Santangeli P, Marchlinski FE. Substrate mapping for unstable ventricular tachycardia. *Heart Rhythm*. 2016;13:569–583. doi: 10.1016/j.hrthm.2015.09.023
3. Dubois R, Shah AJ, Hocini M, Denis A, Derval N, Cochet H, Sacher F, Bear L, Duchateau J, Jais P, et al. Non-invasive cardiac mapping in clinical practice: application to the ablation of cardiac arrhythmias. *J Electrocardiol*. 2015;48:966–974. doi: 10.1016/j.jelectrocard.2015.08.028
4. Rudy Y, Lindsay BD. Electrocardiographic imaging of heart rhythm disorders: from bench to bedside. *Card Electrophysiol Clin*. 2015;7:17–35. doi: 10.1016/j.ccep.2014.11.013
5. Wang Y, Rudy Y. Application of the method of fundamental solutions to potential-based inverse electrocardiography. *Ann Biomed Eng*. 2006;34:1272–1288. doi: 10.1007/s10439-006-9131-7
6. Oster HS, Taccardi B, Lux RL, Ershler PR, Rudy Y. Electrocardiographic imaging: noninvasive characterization of intramural myocardial activation from inverse-reconstructed epicardial potentials and electrograms. *Circulation*. 1998;97:1496–1507. doi: 10.1161/01.cir.97.15.1496
7. Burnes JE, Taccardi B, Rudy Y. A noninvasive imaging modality for cardiac arrhythmias. *Circulation*. 2000;102:2152–2158. doi: 10.1161/01.cir.102.17.2152
8. Cluitmans M, Brooks DH, MacLeod R, Dössel O, Guillem MS, van Dam PM, Svehlikova J, He B, Sapp J, Wang L, et al. Validation and opportunities of electrocardiographic imaging: from technical achievements to clinical applications. *Front Physiol*. 2018;9:1305. doi: 10.3389/fphys.2018.01305
9. Jamil-Copley S, Bokan R, Kojodjojo P, Qureshi N, Koa-Wing M, Hayat S, Kyriacou A, Sandler B, Sohaib A, Wright I, et al. Noninvasive electrocardiographic mapping to guide ablation of outflow tract ventricular arrhythmias. *Heart Rhythm*. 2014;11:587–594. doi: 10.1016/j.hrthm.2014.01.013
10. Erkapic D, Greiss H, Pajitnev D, Zaltsberg S, Deubner N, Berkowitsch A, Möllman S, Sperzel J, Rolf A, Schmitt J, et al. Clinical impact of a novel

three-dimensional electrocardiographic imaging for non-invasive mapping of ventricular arrhythmias-a prospective randomized trial. *Europace*. 2015;17:591–597. doi: 10.1093/europace/euu282
11. Robinson CG, Samson PP, Moore KMS, Hugo GD, Knutson N, Mutic S, Goddu SM, Lang A, Cooper DH, Faddis M, et al. Phase I/II trial of electrophysiology-guided noninvasive cardiac radioablation for ventricular tachycardia. *Circulation*. 2019;139:313–321. doi: 10.1161/CIRCULATIONAHA.118.038261
12. Cuculich PS, Schill MR, Kashani R, Mutic S, Lang A, Cooper D, Faddis M, Gleva M, Noheria A, Smith TW, et al. Noninvasive cardiac radiation for ablation of ventricular tachycardia. *N Engl J Med*. 2017;377:2325–2336. doi: 10.1056/NEJMoa1613773
13. Wang Y, Cuculich PS, Zhang J, Desouza KA, Vijayakumar R, Chen J, Faddis MN, Lindsay BD, Smith TW, Rudy Y. Noninvasive electroanatomic mapping of human ventricular arrhythmias with electrocardiographic imaging. *Sci Transl Med*. 2011;3:98ra84. doi: 10.1126/scitranslmed.3002152
14. Graham AJ, Orini M, Zacur E, Dhillon G, Daw H, Srinivasan NT, Lane JD, Cambridge A, Garcia J, O'Reilly NJ, et al. Simultaneous comparison of electrocardiographic imaging and epicardial contact mapping in structural heart disease. *Circ Arrhythm Electrophysiol*. 2019;12:e007120. doi: 10.1161/CIRCEP.118.007120
15. Sosa E, Scanavacca M, d'Avila A, Pilleggi F. A new technique to perform epicardial mapping in the electrophysiology laboratory. *J Cardiovasc Electrophysiol*. 1996;7:531–536. doi: 10.1111/j.1540-8167.1996.tb00559.x
16. Tung R, Mathuria N, Michowitz Y, Yu R, Buch E, Bradfield J, Mandapati R, Wiener I, Boyle N, Shivkumar K. Functional pace-mapping responses for identification of targets for catheter ablation of scar-mediated ventricular tachycardia. *Circ Arrhythm Electrophysiol*. 2012;5:264–272. doi: 10.1161/CIRCEP.111.967976
17. de Chillou C, Groben L, Magnin-Poull I, Andronache M, MagdiAbbas M, Zhang N, Abdelaal A, Ammar S, Sellal JM, Schwartz J, et al. Localizing the critical isthmus of postinfarct ventricular tachycardia: the value of pace-mapping during sinus rhythm. *Heart Rhythm*. 2014;11:175–181. doi: 10.1016/j.hrthm.2013.10.042
18. Coronel R, de Bakker JM, Wilms-Schopman FJ, Opthof T, Linnenbank AC, Belterman CN, Janse MJ. Monophasic action potentials and activation recovery intervals as measures of ventricular action potential duration: experimental evidence to resolve some controversies. *Heart Rhythm*. 2006;3:1043–1050. doi: 10.1016/j.hrthm.2006.05.027
19. Orini M, Taggart P, Lambiase PD. *In vivo* human sock-mapping validation of a simple model that explains unipolar electrogram morphology in relation to conduction-repolarization dynamics. *J Cardiovasc Electrophysiol*. 2018;29:990–997. doi: 10.1111/jce.13606
20. Rudy Y, Burnes JE. Noninvasive electrocardiographic imaging. *Ann Noninvasive Electrocardiol*. 1999;4:340–359.
21. Orini M, Taggart P, Srinivasan N, Hayward M, Lambiase PD. Interactions between activation and repolarization restitution properties in the intact human heart: in-vivo whole-heart data and mathematical description. *PLoS One*. 2016;11:e0161765. doi: 10.1371/journal.pone.0161765
22. Martin CA, Orini M, Srinivasan NT, Bhar-Amato J, Honarbakhsh S, Chow AW, Lowe MD, Ben-Simon R, Elliott PM, Taggart P, et al. Assessment of a conduction-repolarisation metric to predict arrhythmogenesis in right ventricular disorders. *Int J Cardiol*. 2018;271:75–80. doi: 10.1016/j.ijcard.2018.05.063
23. Andreu D, Fernández-Armenta J, Acosta J, Penela D, Jáuregui B, Soto-Iglesias D, Syrovnev V, Arbelo E, Tolosana JM, Berruezo A. A QRS axis-based algorithm to identify the origin of scar-related ventricular tachycardia in the 17-segment American Heart Association model. *Heart Rhythm*. 2018;15:1491–1497. doi: 10.1016/j.hrthm.2018.06.013
24. Gepstein L, Hayam G, Ben-Haim SA. A novel method for nonfluoroscopic catheter-based electroanatomical mapping of the heart. *In vitro* and *in vivo* accuracy results. *Circulation*. 1997;95:1611–1622. doi: 10.1161/01.cir.95.6.1611
25. Duchateau J, Sacher F, Pambrun T, Derval N, Chamorro-Servent J, Denis A, Ploux S, Hocini M, Jaïs P, Bernus O, et al. Performance and limitations of noninvasive cardiac activation mapping. *Heart Rhythm*. 2019;16:435–442. doi: 10.1016/j.hrthm.2018.10.010
26. Sapp JL, Dawoud F, Clements JC, Horácek BM. Inverse solution mapping of epicardial potentials: quantitative comparison with epicardial contact mapping. *Circ Arrhythm Electrophysiol*. 2012;5:1001–1009. doi: 10.1161/CIRCEP.111.970160
27. Cluitmans MJM, Bonizzi P, Karel JMH, Das M, Kietselaer BLJH, de Jong MMJ, Prinzen FW, Peeters RLM, Westra RL, Volders PGA. *In vivo* validation of electrocardiographic imaging. *JACC Clin Electrophysiol*. 2017;3:232–242. doi: 10.1016/j.jacep.2016.11.012
28. Ghanem RN, Jia P, Ramanathan C, Ryu K, Markowitz A, Rudy Y. Noninvasive electrocardiographic imaging (ECGI): comparison to intraoperative mapping in patients. *Heart Rhythm*. 2005;2:339–354. doi: 10.1016/j.hrthm.2004.12.022
29. Revishvili AS, Wissner E, Lebedev DS, Lemes C, Deiss S, Metzner A, Kalinin VV, Sopov OV, Labartkava EZ, Kalinin AV, et al. Validation of the mapping accuracy of a novel non-invasive epicardial and endocardial electrophysiology system. *Europace*. 2015;17:1282–1288. doi: 10.1093/europace/euu339
30. Ramanathan C, Jia P, Ghanem R, Calvetti D, Rudy Y. Noninvasive electrocardiographic imaging (ECGI): application of the generalized minimal residual (GMRes) method. *Ann Biomed Eng*. 2003;31:981–994. doi: 10.1114/1.1588655
31. Oster HS, Taccardi B, Lux RL, Ershler PR, Rudy Y. Noninvasive electrocardiographic imaging: reconstruction of epicardial potentials, electrograms, and isochrones and localization of single and multiple electrocardiac events. *Circulation*. 1997;96:1012–1024. doi: 10.1161/01.cir.96.3.1012
32. Bear LR, LeGrice IJ, Sands GB, Lever NA, Loiselle DS, Paterson DJ, Cheng LK, Smaill BH. How accurate is inverse electrocardiographic mapping? *Circ Arrhythmia Electrophysiol*. 2018; 11:e006108. doi: 10.1161/CIRCEP.117.006108
33. Burnes JE, Taccardi B, Ershler PR, Rudy Y. Noninvasive electrocardiogram imaging of substrate and intramural ventricular tachycardia in infarcted hearts. *J Am Coll Cardiol*. 2001;38:2071–2078. doi: 10.1016/s0735-1097(01)01653-9
34. Bear LR, Huntjens PR, Walton RD, Bernus O, Coronel R, Dubois R. Cardiac electrical dyssynchrony is accurately detected by noninvasive electrocardiographic imaging. *Heart Rhythm*. 2018;15:1058–1069. doi: 10.1016/j.hrthm.2018.02.024
35. Stevenson WG, Khan H, Sager P, Saxon LA, Middlekauff HR, Natterson PD, Wiener I. Identification of reentry circuit sites during catheter mapping and radiofrequency ablation of ventricular tachycardia late after myocardial infarction. *Circulation*. 1993;88(4 pt 1):1647–1670. doi: 10.1161/01.cir.88.4.1647
36. Cluitmans MJ, Peeters RL, Westra RL, Volders PG. Noninvasive reconstruction of cardiac electrical activity: update on current methods, applications and challenges. *Neth Heart J*. 2015;23:301–311. doi: 10.1007/s12471-015-0690-9